ANNUAL TECHNICAL REPORT

NASA Contract NAS8-34383

CONTAINERLESS HIGH TEMPERATURE PROPERTY MEASUREMENTS BY ATOMIC FLUORESCENCE

by

Paul C. Nordine, Principal Investigator

and

Robert A. Schiffman, Research Associate

Department of Chemical Engineering
Yale University
P. O. Box 2159 Yale Station
New Haven, CT 06520

October, 1982

Prepared for:

Materials Processing in Space Program

Contract Monitor:

R. Fallon, LA11
NASA-George C. Marshall Space Flight Center
Marshall Space Flight Center, Alabama 35812

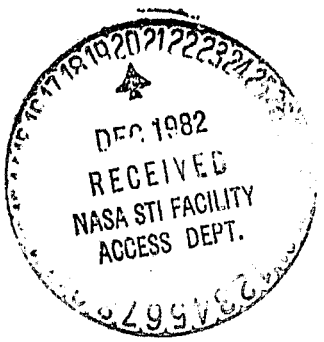

CONTENTS

TABLES

FIGURES

FIGURES (continued)

I. INTRODUCTION

The purposes of this research include the developement of laser induced fluorescence techniques for the containerless study of high temperature processes and material properties and of levitation and heating techniques for containerless earth-based experimentation, and the application of these methods in containerless study of high temperature material, thermodynamic, transport, and other properties, including temperature.

During the period, June 15, 1981 to the present, we have assembled the apparatus, completed various design changes that the initial experiments[1] suggested, and carried out experiments in which fluorescence of atomic aluminum, mercury, or tungsten were studied. These experiments include measurements of:

1. Al atom evaporation from CW CO_2 laser heated and aerodynamically levitated sapphire and alumina spheres, and self-supported sapphire filaments,
2. Al atom reaction with ambient oxygen in the wake of a levitated specimen,
3. Hg atom concentrations in the wake of levitated alumina and sapphire spheres, relative to the ambient Hg atom concentration,
4. Hg atom concentrations in supersonic levitation jets,
5. metastable, electronically excited W atom concentrations produced by evaporation of an electrically heated tungsten filament.

A brief description of the apparatus, and presentation of the results of the experiments is given below. More detailed presentations will become available as the papers describing our work are completed and submitted for publication.

II. EXPERIMENTAL

The apparatus used in this research is illustrated in Figures 1 and 2 and the photograph for which Table I identifies the labeled components. In the experiments reported, a pulsed dye laser was used to produce fluorescence from atomic mercury, aluminum and tungsten. The Hg-atoms were added to the argon flow. Al atoms were produced by evaporation from CW CO_2 laser heated and aerodynamically levitated sapphire or polycrystalline Al_2O_3 spheres or self supported sapphire filaments. W atoms were evaporated from electrically heated metal filaments. Laser beam and detector aperture positioning devices were used to fix the position at which fluorescence was measured to about 0.01 mm.

III. RESULTS

1. Hg-Atom Fluorescence Study of the Aerodynamic Levitation Jet

The addition of atomic mercury to the argon stream allows the density and velocity of the levitation jet to be measured. Density is obtained, relative to the ambient density, from the ratio of the fluorescent intensity at the point of interest to that at a point outside the jet, under the known ambient conditions. Velocity can be determined[2] by measuring the location of the fluorescent image vs the delay time between a trigger signal from the laser and the interval sampled by the boxcar averager.

Figure 3 presents the Hg fluorescence intensity vs height at the center of the jet for two different delay times, with the location of the focused dye laser beam fixed. It can be seen that the center of the fluorescent image moves about 0.1 mm when the delay time is increased 175 ns. The radiative lifetime of atomic Hg is about 100

ns, and the fluorescence intensity becomes too small for accurate measurement of the image profile at much longer delay times. Figure 4 plots several measurements of the location of the center of the fluorescent image vs delay time. A least-squares analysis gives the velocity, $u = 394 \pm 24$ m/s. Fewer height vs delay time data were obtained for most of the velocities reported below, and these velocity measurements are, therefore, not as precise as that given in this example.

Figure 5 plots several measurements of the radial concentration variation in the jet, at fixed stagnation conditions but different ambient pressures. The density at the jet center was measured relative to the ambient density vs pressure at a larger number of points to give the results in the bottom panel of Figure 6. The top panel of Figure 6 presents jet densities under nearly identical conditions that have been calculated from pitot tube measurements of the jet stagnation pressure (Ref. 3, Fig. 7, curve number 4). Fluorescence measurements under other conditions also give results that agree well with the pitot tube pressure measurements of Ref. 3. Figure 6 reveals oscillations in the jet density with the ambient pressure that were not detected by the pitot tube measurements[3]. These variations of density with pressure may be related to changes in the free jet shock structure that occur as the nozzle expansion ratio is changed. For example, the number of normal shocks that occur in the free jet expansion process is expected to increase as the pressure decreases. We postulate that incremental changes in the number of shocks occur at the pressures at which the jet density decreases with a decrease in the pressure. This will be checked by fluorescence

measurements of the free jet shock structure near the nozzle.

Figure 7 plots the radial variation in jet velocity that was obtained in two ways. The squares present direct measurements by the delayed fluorescence technique. The circles are calculated from density measurements and the assumptions that i) the jet is adiabatic, ii) the pressure is uniform, and iii) the Hg-atom concentration is proportional to argon density, i.e., no heavy atom inertial separation effects occur in the free-jet expansion process, so that the Hg-atom mole fraction is uniform. The density-temperature product is then constant so the density measurements give local temperatures from the known ambient temperature. The kinetic energy of gas flow equals $C_p(T_0 - T)$ where T_0 and T are the stagnation and calculated jet temperatures, respectively. It can be seen that the jet velocity profile calculated under the above assumptions agrees well with that measured by the delayed fluorescence technique.

A further check can be made on the above analysis. If the pressure is uniform and equals the ambient pressure, the jet momentum flow rate is:

$$mu = m^*u^* + A^*(p^* - p), \tag{1}$$

where * refers to choked conditions. The value of mu can also be calculated from:

$$mu = 2\pi\int_0^\infty \rho\, u^2 r dr, \tag{2}$$

where ρ is gas density. For this experiment, Equation (1) gives mu = 791 g cm/s^2 and Equation (2) gives mu = 843 g cm/s^2. When the same check is applied to the data of Figure 5, the results presented in Table II are obtained. It is apparent from these results that one (or more) of the assumptions stated above is not always correct. Velocity

measurements by delayed fluorescence may give further insight into jet behavior but have not yet been completed. Also, potassium atom fluorescence may be employed to eliminate heavy atom separation effects. Nevertheless, this fluorescence study of jet behavior provides good support for the model of supersonic jet levitation that is given in Ref. 3.

2. Al-Atom Fluorescece: Sapphire and Alumina Evaporation

A. Sapphire Filament

Aerodynamically levitated spheres become unstable when they begin to melt. However, a self-supported sapphire filament can be partially melted. The effective total emittance of liquid Al_2O_3 is greater than that of the solid and laser power necessary to mel. through a sapphire filament is about six times that required to bring the solid to the melting temperature. The effective spectral emittance of the liquid is also greater than that of the solid and the apparent temperature of a partially molten sapphire filament increases as the fraction of liquid material increases, at constant true temperature. These effects were studied by measuring the Al-atom fluorescence intensity in the wake of a laser heated sapphire filament vs apparent specimen temperature. The results are illustrated in Figure 8, which shows a nearly constant intensity at T_a > 1480K, where the specimen begins to melt. The small increase of intensity with apparent temperature above 1480K is mainly due to a larger evaporation coefficient for the liquid than for the solid and an increase in the evaporating area with the fraction of the specimen that is liquid, due to a volume difference between solid and liquid Al_2O_3.

B. Levitated Sapphire and Alumina Spheres

The spectral emittance of polycrystalline alumina is greater than that of sapphire. Thus, a greater heating laser power is necessary to bring an alumina sphere to a given temperature than is required for a sapphire sphere at the same temperature. At equal temperatures, the alumina sphere also has a greater spectral emittance and apparent temperature. But the vapor pressure at equal temperatures is the same for alumina and sapphire. The Al-atom fluorescent intensity in the wake of levitated 0.318 cm alumina and sapphire spheres is illustrated in Figure 9 as a function of apparent specimen temperature. For each specimen, a constant intensity is approached at the highest temperatures, when the specimen begins to melt. That is, the maximum intensities are achieved at the same true temperatures. The apparent temperature differences at equal true temperatures can thus be read from the Figure, at points where each specimen gave equal fractions of the maximum intensity.

The relation between specimen emittance, e, true temperature, T, and apparent temperature, T_a is

$$1/T - 1/T_a = \lambda C_2 \ln(e), \qquad (3)$$

where λ = 0.66 micrometer is the effective pyrometer wavelength and C_2 = 14388 micrometer(degree K). The results of Figure 9 yield an effective alumina:sapphire emittance ratio equal to 16 for spheres of 0.318 cm diameter. Extrapolation of the linear lower temperature data on sapphire to the melting point gives an apparent melting temperature equal to 1460K, where the true temperature is 2327K. The emittance of the sapphire sphere is thus about 0.0038, at temperatures above about 1800K. This value is less than would be calculated from the apparent

melting temperature of the sapphire filament, probably because the sapphire filament contained internal voids that scatter light and produce a larger emittance than would be observed for a more perfect crystal.

Al-atom fluorescence data were also obtained with 0.4 and 0.5 cm diameter sapphire spheres. All of the data for levitated sapphire spheres yield a single intensity vs temperature curve if the data are normalized by the maximum intensities for each data set and the apparent temperatures are adjusted according to the equation

$$1/T_{a,d'} - 1/T_{a,d} = \lambda/C_2 \ln(d/d') \qquad (4)$$

in which the emittance has been taken proportional to specimen diameter, and apparent temperature measurements corrected to a nominal diameter, d'. This result shows that the emittance of sapphire is determined by bulk emission from the solid and that the contribution of any additional emmission of light from the surface of the specimen is negligible.

C. Al-atom Reaction with Ambient Oxygen or Water

When a new alumina or sapphire specimen is first placed in the apparatus, the Al-atom intensities measured a few mm from the specimen surface in the wake of the heated specimen are 10 - 100 times less than would be expected. After overnight pumping on the apparatus, reproducable higher fluorescence intensities were obtained. Also, if the Al-atom fluorescence intensity was measured vs height above the levitated specimen and extrapolated to the specimen surface, reproducable measurements were obtained. These effects are caused by the reaction of evaporating Al-atoms with ambient water or oxygen, which outgasses from the surfaces of the apparatus after it has been

opened to the atmosphere. With oxygen, the reaction would be

$$Al(g) + O_2(g) = AlO(g) + O(g),$$

a bimolecular exchange reaction whose rate constant should have a value about 10^{-10} cm^3/moleule sec.

Figure 10 plots the variation of intensity with height above the specimen for different values of the ambient oxygen partial pressure that were set by adding oxygen to the levitating argon gas. The greater expected rate of Al consumption for greater ambient oxygen concentration is found. Unequal intensities at zero height do not occur after corrections for small sensitivity differences between the experiments are applied to the data. The rates of Al loss in the specimen wake are less than would be expected from the rate constant estimated above and the assumption that Al transport in the wake of the specimen is by diffusion alone. These phenomena will be discussed further in a publication on Al-atom fluorescence studies now in preparation.

3. Hg-Atom Fluorescence Gas Thermometry

In ideal gas thermometry, the gas densities at two points in an apparatus are measured under static conditions. With uniform pressure and a known value for one of the temperatures, the other temperature can be calculated because the product of density and temperature is constant for an ideal gas. The same principal can be used to measure very high temperatures that are not amenable to conventional ideal gas thermometry, using laser induced fluorescence to obtain the gas density ratio. In the experiments we have carried out Hg-atom density ratios were measured, with Hg as the fluorescing seed gas in argon. Here, the product of Hg concentration and temperature cannot be

assumed constant because thermal diffusion effects and inertial separation of heavy and light gases may occur.

The ambient Hg-atom fluorescence intensity was first measured under the flow conditions that occur in levitation experiments. Then sapphire and alumina spheres were levitated and heated, and the Hg-atom fluorescence intensity measured at a point 0.9 mm above the specimen in the specimen wake. The ambient to high temperature Hg-atom concentration ratios are plotted vs the apparent specimen temperature to ambient temperature ratios in Figure 11. The left panel gives the sapphire and alumina data at the apparent temperatures that were actually measured for these specimens. In the right hand panel of the figure, the sapphire data have been adjusted to higher temperatures, according to the temperature corrections that are deduced from the Al-atom fluorescence data in Figure 9. The ambient temperatures were between 305 - 320K. It can be seen that the temperature adjusted sapphire data agree with the alumina data to about ± 50K.

A small systematic departure of the temperature adjusted sapphire data from the line drawn through the alumina data appears at temperature ratios greater than about 5.2. This error may arise from differences in the thermal diffusion effects for the two experiments. Alumina specimens require a greater laser power to achieve a given temperature than do sapphire specimens, and the apparatus achieves a greater ambient temperature for the alumina than for the sapphire experiments.

4. W-Atom Fluorescence: Tungsten Filament Evaporation

A partial energy level diagram for atomic tungsten is given in

Figure 12. The light vertical lines drawn on the diagram indicate the transitions that were observed in a brief survey in the wavelength range between 391 - 411 nm. The solid lines indicate the transitions employed to study the temperature dependence of metastable atom concentration for four different electronic states. For these measurements, fluorescence was excited at one wavelength and observed at another, by monitoring emission for the transitions indicated by dashed lines in the figure.

The tungsten evaporation data are given in Figure 13. This experiment was carried out at low pressure, where intensity is proportional to evaporation rate. The departure of the log I vs 1/T data from straight lines at the highest temperatures may therefore reveal a decrease in the evaporation coefficient with temperature. This effect could also have other explanations. The high range of the optical pyrometer that was used needs to be calibrated. Also, the concentration at the point sampled in the filament wake depends on the rate of diffusive spreading from the (line) filament source, and on the temperature of the gas. The dependence of wake gas temperature on specimen temperature may change with temperature if the argon-tungsten thermal accomodation coefficient changes rapidly with temperature in the range of the experiment. Pyrometer calibration and further experiments at higher ambient temperatures should resolve some of these questions. However, the 0.025 cm filament evaporation rate is sufficient that the experiment duration is limited to about 10 minutes at the highest temperatures. Further study of tungsten evaporation will probably employ electromagnetically levitated specimens.

IV. DISCUSSION

Sensitivity and Precision of Measurements

The sensitivity of experiments with Al and W atom fluorescence is sufficient to yield atom concentration measurements as low as 2×10^8 cm^{-3}, or pressures ca. 10^{-11} to 10^{-10} atm. A 100-fold increase in sensitivity would be possible if a greater fraction of the light emitted from a larger fluorescing volume were collected. However, reduced spatial resolution of the concentration measurements would then occur.

The precision with which the location of fluorescence measurements can be set is about $\pm$ 10 micrometers, which is the approximate average deviation of points from the line in the height vs delay time data of Fig. 4. Improved precision in velocity measurement could be achieved by use of a fluorescing species whose radiative lifetime was longer than that of Hg, ca. 100 ns. For example, the $4s\ ^2S_{1/2}$ to $np\ ^2P_{1/2,3/2}$ transitions of potassium can be excited with the available equipment. For these transitions, the upper state lifetimes increase with n, to, e.g., 5.0 microseconds at n = 9. Thus, a 10- to 50-fold improvement in velocity measurement precision should be possible.

The use of atomic K as a fluorescing ambient gas would also reduce thermal diffusion and inertial separation effects because the atomic masses of K and Ar are nearly equal. The apparatus temperature would need to be maintained at 50 - 100°C to provide a sufficient potassium vapor pressure. Also, specimen temperatures would be limited to about 1600K because thermal ionization of K-atoms at higher temperatures would significantly influence their concentration.

Temperature Measurement

Three methods for temperature measurement by laser induced fluorescence do not require knowledge about specimen properties such as emittance.

The method of Hg-atom gas thermometry would be applicable to temperatures where Hg-atom ionization begins to occur (> 3000K). Improved accuracy (± 50K in the present work) should be possible if the ambient conditions were precisely controlled between experiments and at different specimen temperatures. In the present work, small variations in pressure, ambient temperature, gas flow rate, and specimen position were unavoidable, that could be eliminated in containerless experiments under a gravity free enviornment. Then, the accuracy of temperature measurements by this method would be limited by the precision of intensity measurements.

The mean thermal velocity of atoms that evaporate from a specimen under vacuum conditions can be measured in the same way that jet velocity was obtained here. Since velocity is proportional to $T^{0.5}$, the precision of temperatures measured in this way would be twice that of velocity measurements. The current work gave a velocity measurements precision equal to 6%. If the evaporating species can be excited to long-lived (ca. 1 microsecond) excited states, a ten fold improvement in velocity measurements should be possible to give temperatures to ± 1.2%.

The third method for temperature measurements would employ the intensity ratio for two different electronic states of a given vapor species. For atomic tungsten, the $^5D_0$ to $^3H_5$ excitation energy is E = 43,100 cal/mole. Taking r as the fluorescence intensity ratio

for transitions involving these states, one has

$$d \ln r = E/RT \, d \ln T \qquad (5)$$

At the melting point of tungsten, 3680K, this becomes

$$dr/r = 5.89 \, dT/T \qquad (6)$$

so that temperature is determined from intensity measurements with a precision 5.89 times that of the intensity ratio. This is the most precise of these methods for temperature measurement by laser induced fluorescence.

Other Experiments

A number of new experiments have been initiated. The emphasis of work with electromagnetic levitation will be on the study of liquid metals and alloys. Temperature measurements that are free of specimen emittance corrections will be employed and the activities of components of binary liquid systems will be investigated. The completion of our fluorescence study of aerodynamic levitation jets will include studies of the shock structure near the free jet nozzle and experiments with atomic potassium that yield more precise velocity measurements. A comparison of K-atom and Hg-atom fluorescence studies of free jet shock structure will demonstrate if heavy atom inertial separation effects occur in the jet.

V. REFERENCES

1. P. C. Nordine, R. A. Schiffman and D. S. Sethi, "Atomic Fluorescence Study of High Temperature Aerodynamic Levitation", in G. E. Rindone, ed., Materials Processing in the Reduced Gravity Enviornment of Space, Elsevier, New York, 1982, pp. 43 - 48.

2. P. C. Nordine and R. A. Schiffman, "Flow Velocity Measurement by Delayed Detection of Laser Induced Fluorescence", NASA New Technology Report, August 5, 1982.

3. P. C. Nordine and R. M. Atkins, "Aerodynamic Levitation of Laser-Heated Solids in Gas Jets", Rev. Sci. Instrum. 53, 1456 (1982).

VI. PUBLICATIONS AND PRESENTATIONS

1-3. See References.

4. R. A. Schiffman and P. C. Nordine, "Containerless High Temperature Property Measurements by Laser Induced Fluorescence", poster presentation at the Gordon Research Conference on High Temperature Chemistry, Tilton, NH, July 26-30, 1982.

5. P. C. Nordine, "Chemical Reaction Studies with Laser Induced Fluorescence", presented at the NASA Containerless Processing Meeting, Washington, D. C., Oct. 21-22, 1982.

Table I

Legend for Photograph: Containerless Property Measurements by Laser Induced Atomic Fluorescence

A.	Chamber with levitated, CW CO_2 laser heated alumina sphere.
B.	Directed infrared laser beam for heating.
C.	Dye laser.
D.	Optical positioning for directing dye laser beam through the levitation apparatus.
E.	Fluorescence focusing mirror.
F.	Fluorescence detector with pinhole aperture.
G.	Detector positioning devices with stepper motor drives.
H.	Optical fiber to monochromator, photodetector and boxcar averager.
I.	Ambient temperature fluorescence intensity measurement chamber.
J.	Ambient detector with optical fiber to second monochromator, photodetector and electronics.
K.	Isothermal flow chamber for adding mercury vapor to argon gas flow.
L.	Stepper motor controller.
M.	Electronic manometer readout for chamber and critical flowmeter.
N.	Power controller for CW CO_2 laser.
P.	Automatic optical pyrometer.
Q.	Throttle valve to vacuum pump.
R.	Induction heater for metal specimen levitation.

ORIGINAL PAGE IS
OF POOR QUALITY

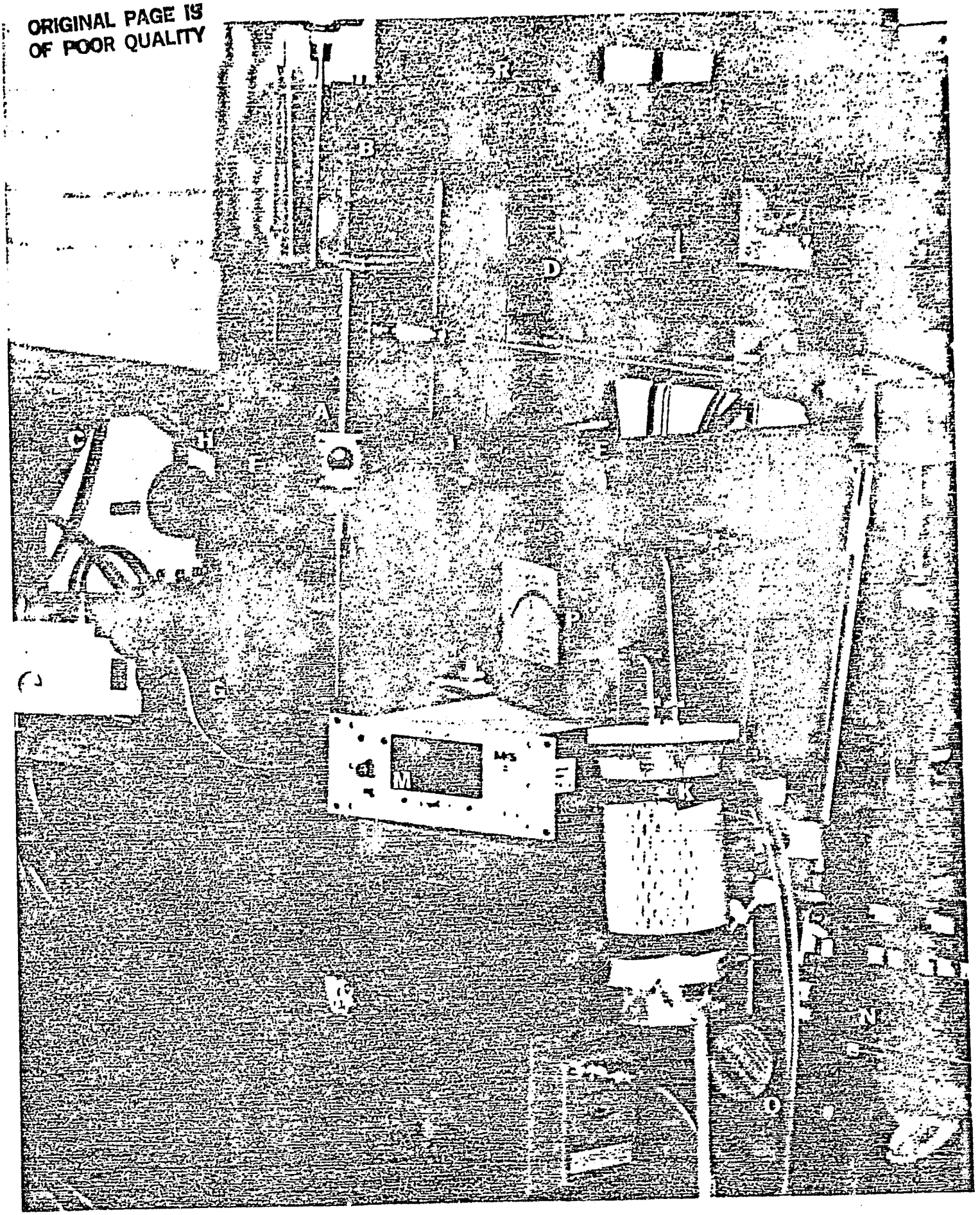

Table II

Jet Momentum Flow Rate For the Experiments of Figure 5

Pressure	Jet Momentum, g cm/s^2		Value Ratio
	Equation (1)	Equation (2)	Eq.(1)/Eq.(2)
3.5	584	553	1.06
5.0	576	641	0.90
7.4	563	579	0.97
10.1	548	499	0.95
19.8	495	273	1.81
30.8	435	365	1.19

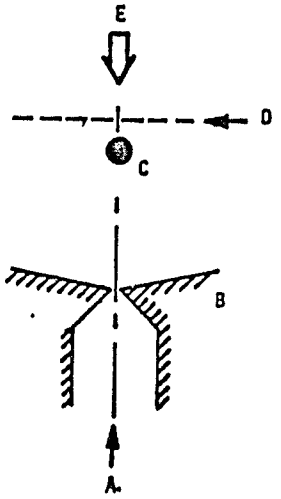

Figure 1 (left). Side View of the Experiment. A - Ar flow, with added Hg if appropriate, B - Nozzle with 0.082 cm diameter throat, C - Levitated specimen, D - Focused dye laser beam, E - CW CO_2 heating laser.

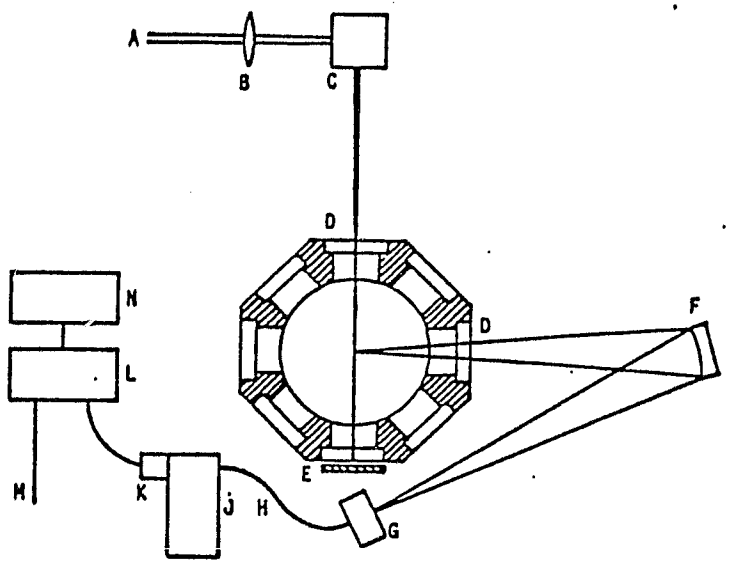

Figure 2 (right). Top view of the apparatus. A - Pulsed laser beam, B - Quartz lens, focal length = 50 cm, C - Beam steering device, D - Quartz windows, E - Laser beam stop, F - Front surface reflective lens, G - 0.40 mm aperture and positioning device, H - uv grade optical fiber, J - 1/4 m monochromator, K - Phototube, L - Boxcar averager, M - Trigger signal from laser, N - Chart recorder.

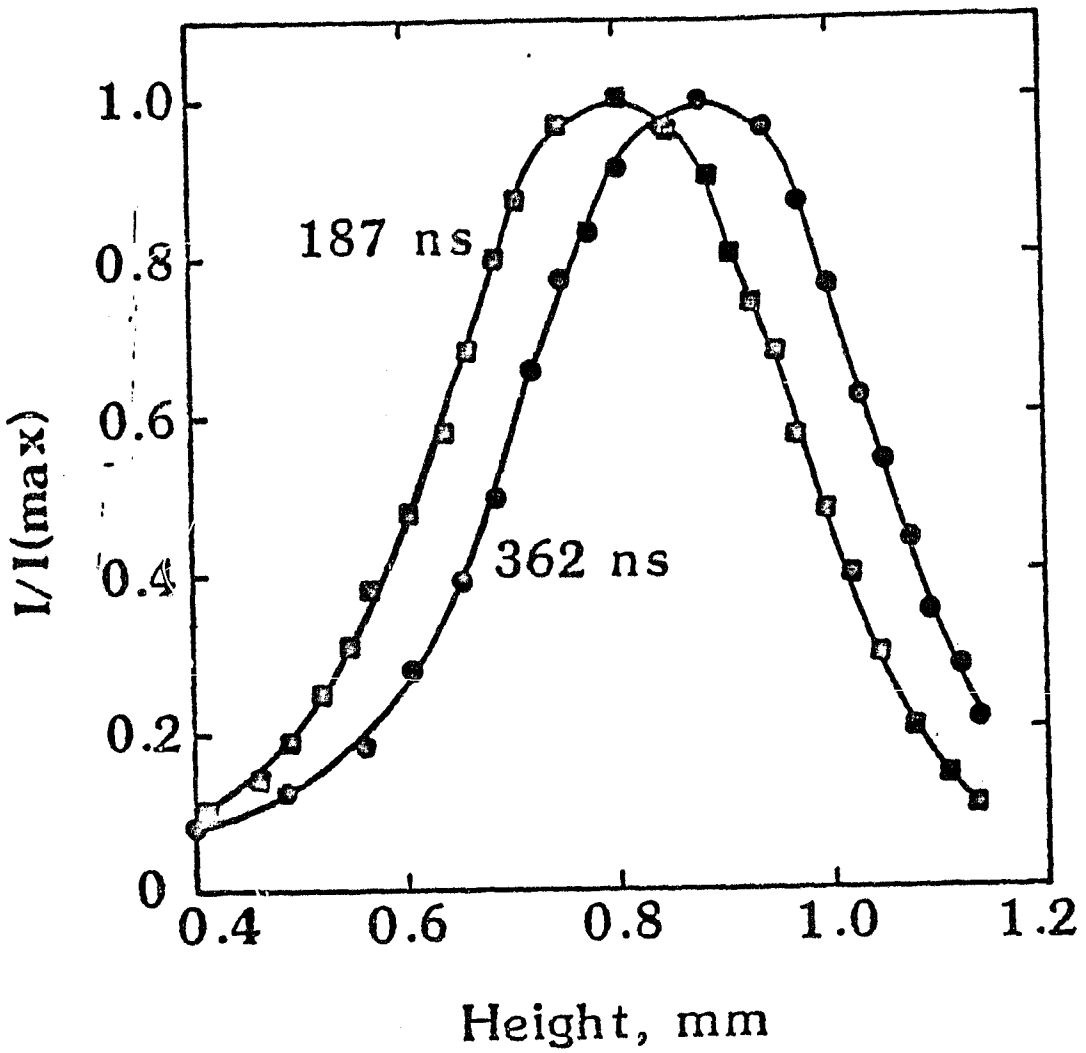

Figure 3. Hg-Atom Fluorescence Intensity vs Detector Aperture Height for two Laser Trigger to Signal Measurement Interval Delay Times. Conditions were: height above nozzle = 2.25 cm, Ar flow rate = 410 cc(STP)/min, p = 3.1 torr, nozzle stagnation pressure, p_0 = 77 torr.

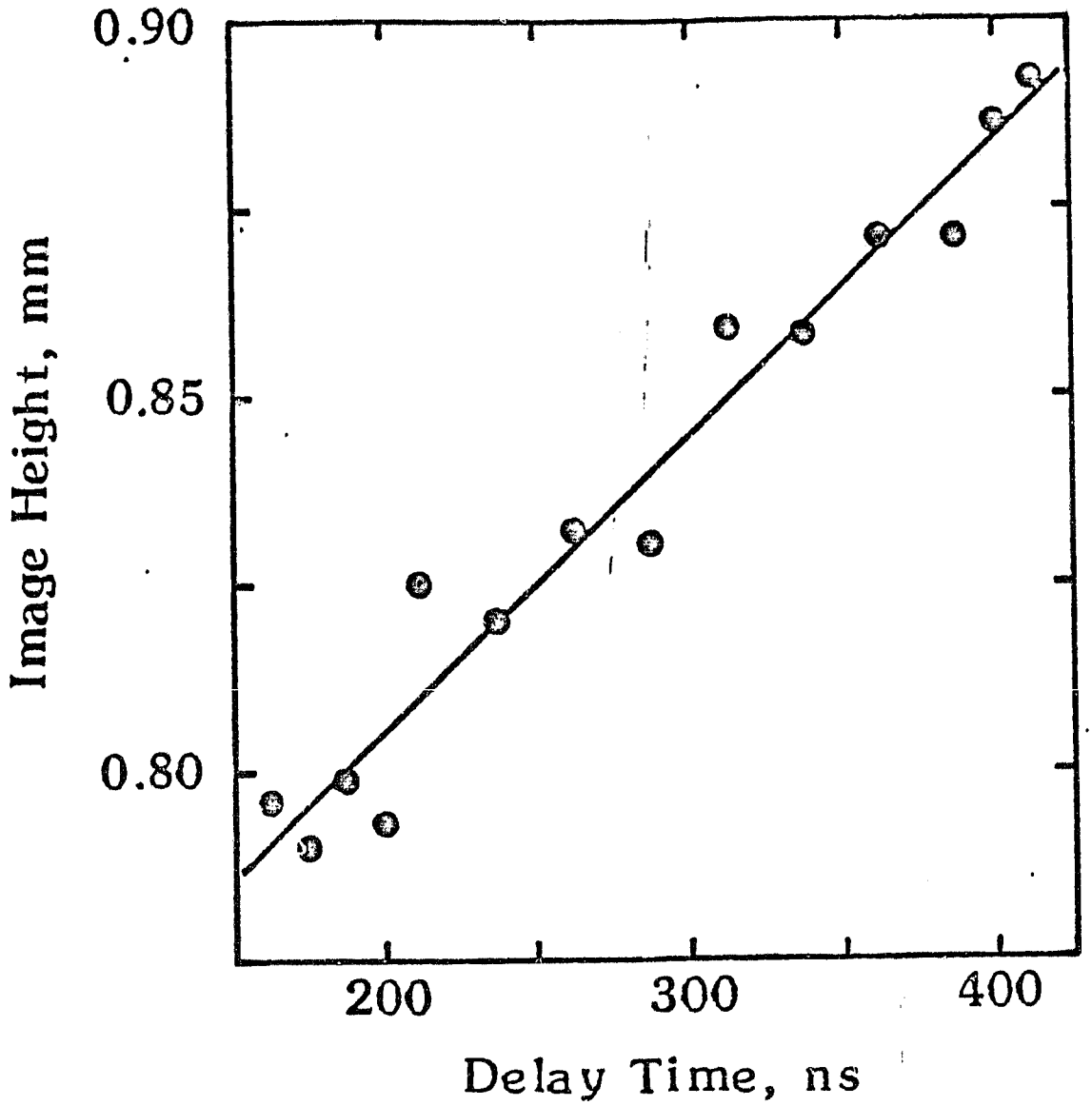

Figure 4. Hg-Atom Fluorescence Image Height vs Signal Detection Delay Time. Slope = 394 ± 24 m/s. Same conditions as in Figure 3.

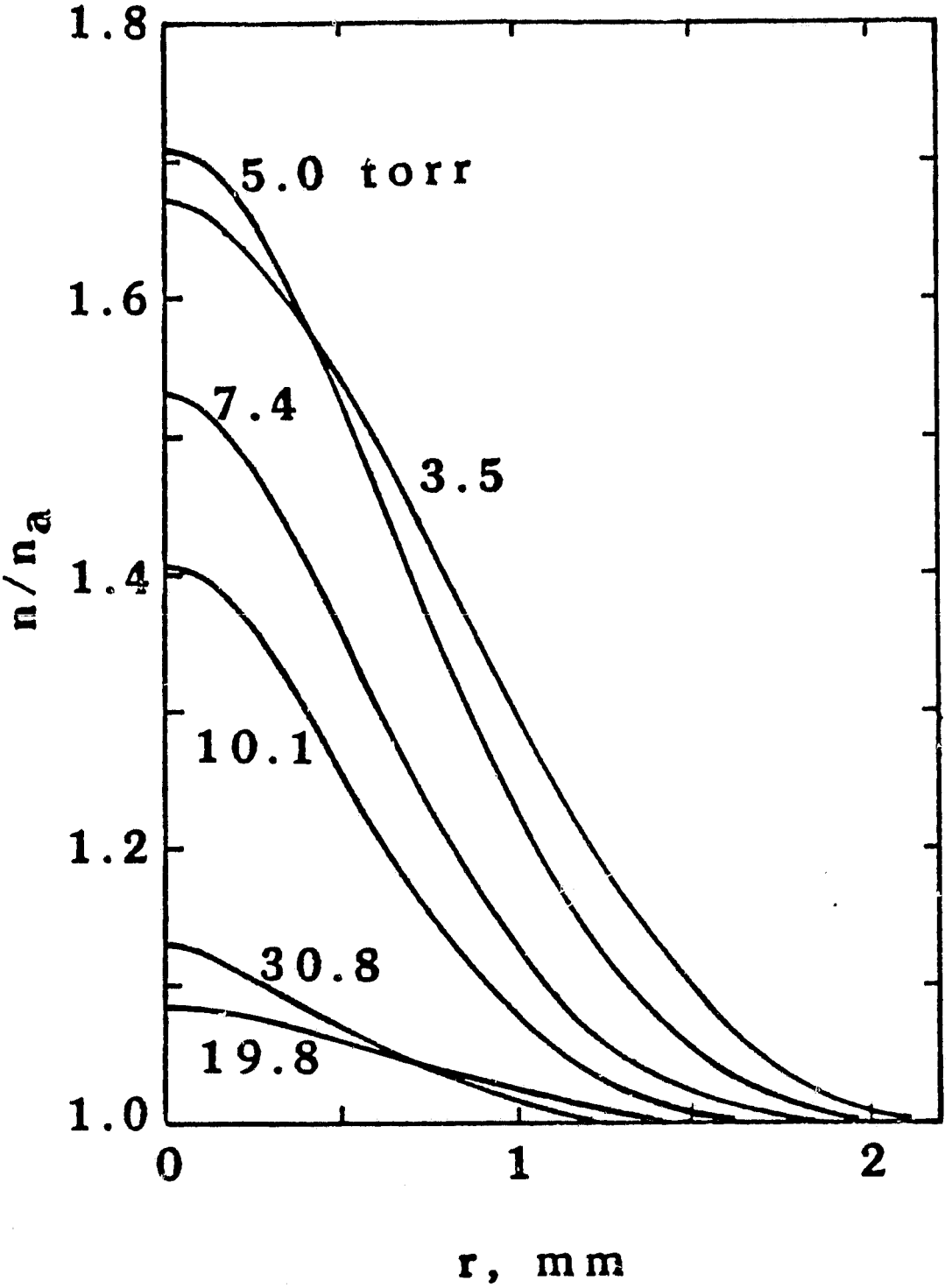

Figure 5. Radial Variation of Concentration in a Free Jet at Different Ambient Pressures. Conditions are: height above nozzle = 2.00 cm, Ar flow rate = 455 cc(STP)/min, p_0 = 85 torr.

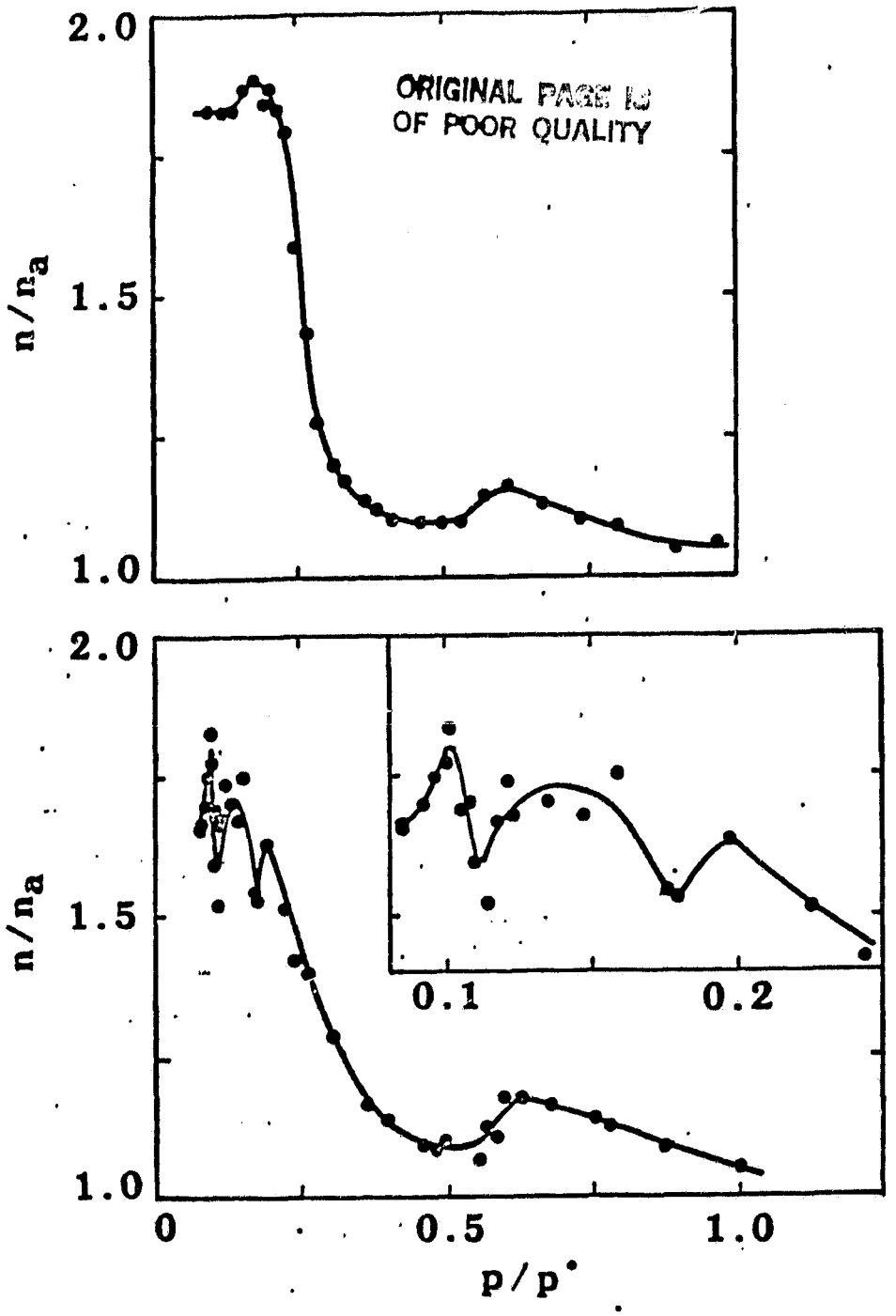

Figure 6. Density at Jet Center vs Ambient Pressure. p* = pressure at (choked) nozzle. The upper panel gives data calculated from pitot tube measurements[3]. The lower panel and insert give measurements by the Hg-atom fluorescence technique.

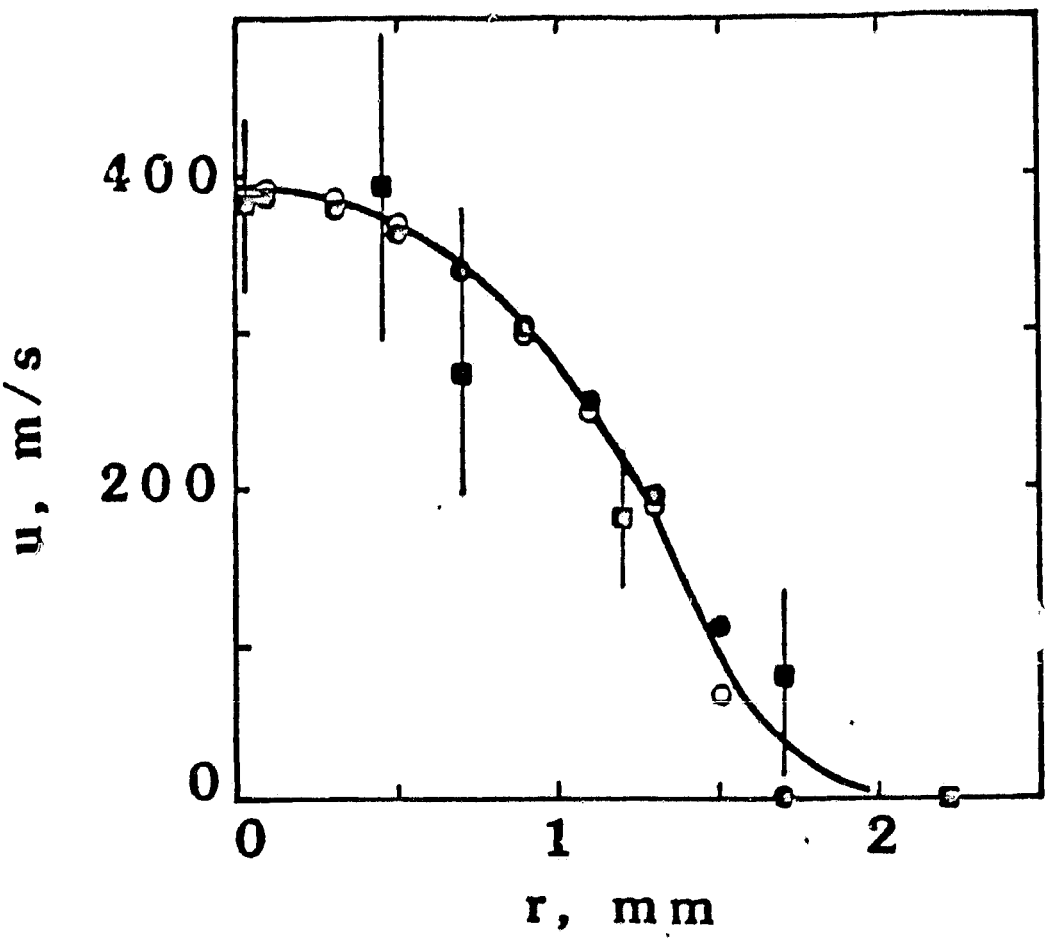

Figure 7. Radial Variation of Free Jet Velocity. Squares give direct measurements by the delayed fluorescence technique. Circles are calculated from density measurements and assumptions that the flow is adiabatic, the pressure is uniform, and that no heavy atom (Hg)/light atom (Ar) separation effects occur. Conditions are: height above nozzle = 1.65 cm, Ar flow rate = 624 cc(STP)/min, p_0 = 115 torr, and p = 5.1 torr.

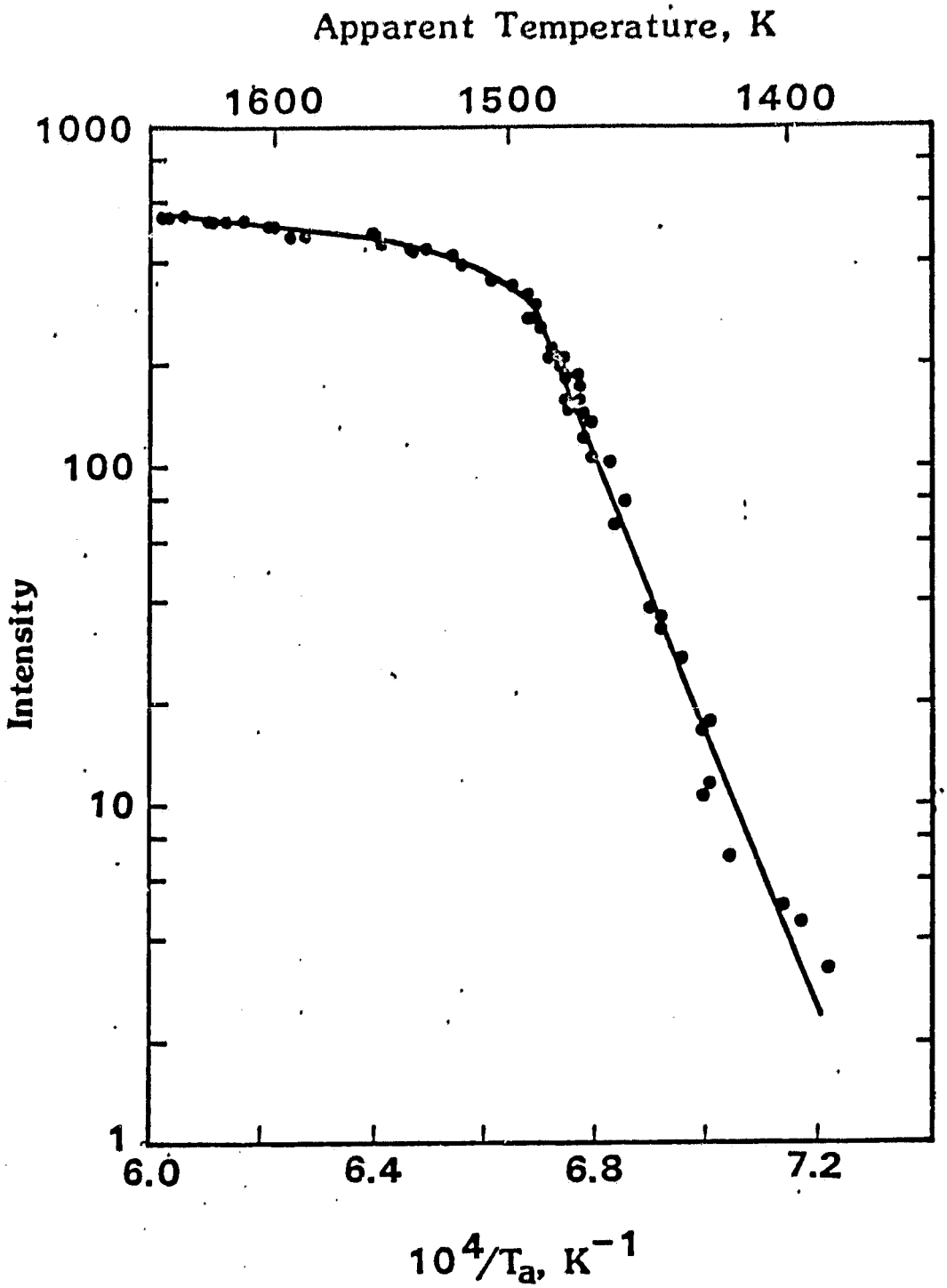

Figure 8. Al-Atom Fluorescence Intensity vs Apparent Temperature for Laser Heated Sapphire Filament.

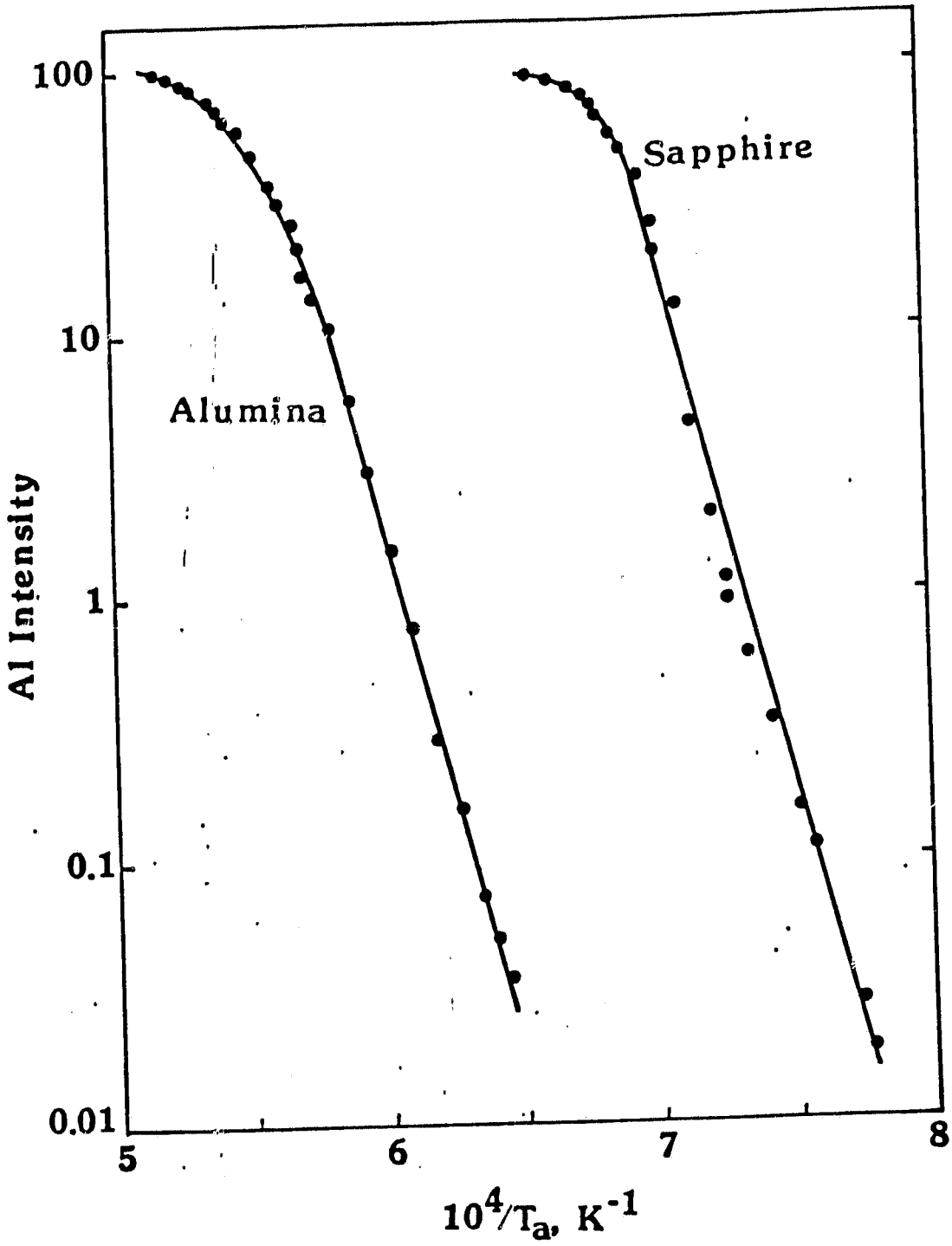

Figure 9. Al-Atom Fluorescence Intensity vs Apparent Temperature for Levitated Spheres.

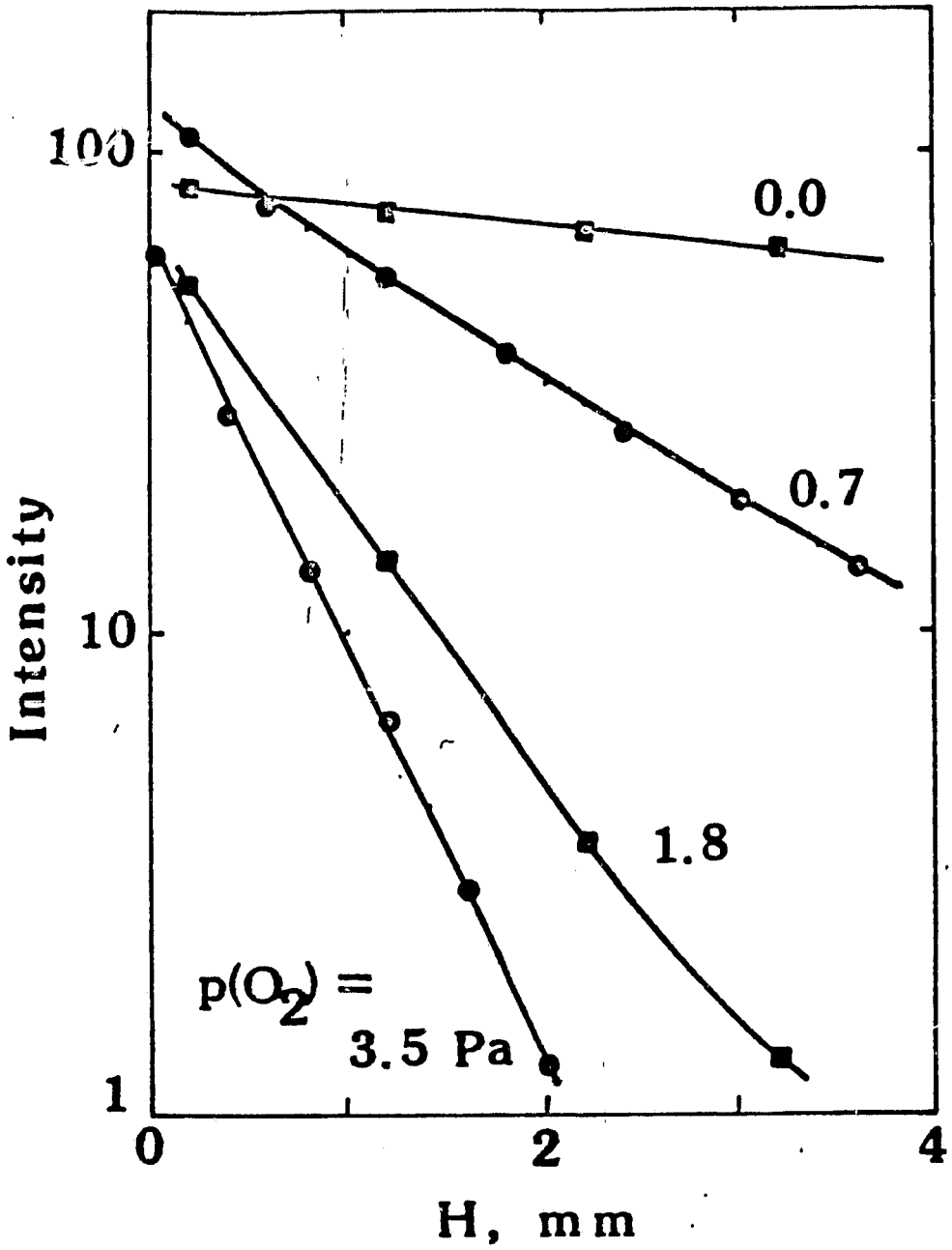

Figure 10. Al-Atom Fluorescence Intensity vs Height Above a Levitated Sapphire Sphere.

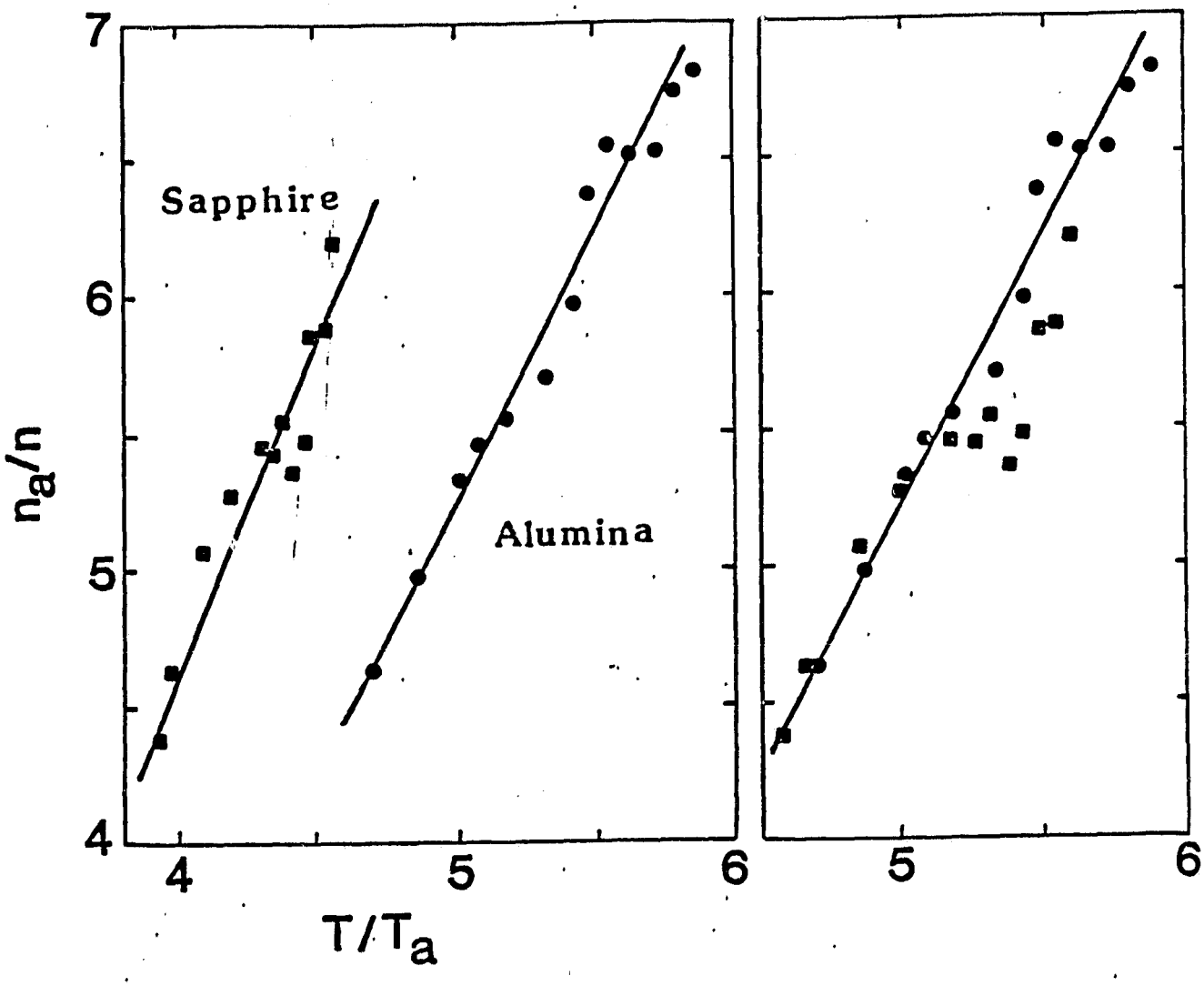

Figure 11. Test of Hg-Atom Fluorescence Thermometry. Ambient to high temperature Hg-atom concentration ratio vs apparent specimen temperature to ambient temperature ratio. In the right hand panel, the sapphire data are plotted at temperature ratios adjusted according to the sapphire to alumina temperature corrections deduced from Al-atom fluorescence measurements over levitated sapphire and alumina spheres.

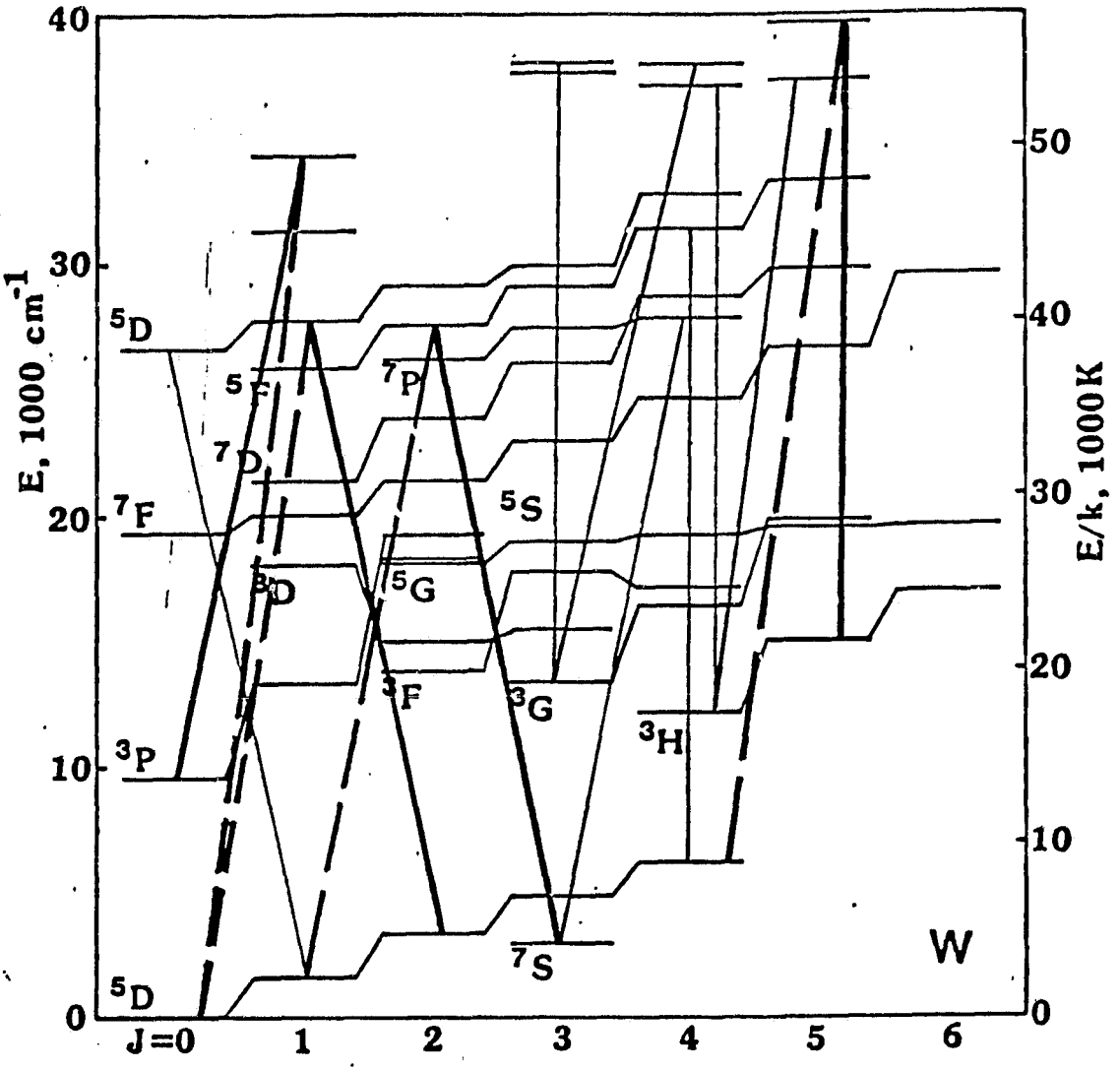

Figure 12. Partial Energy Level Diagram for Atomic Tungsten. The light lines indicate observed transitions. The heavy lines indicate transitions for which intensity vs temperature data have been obtained.

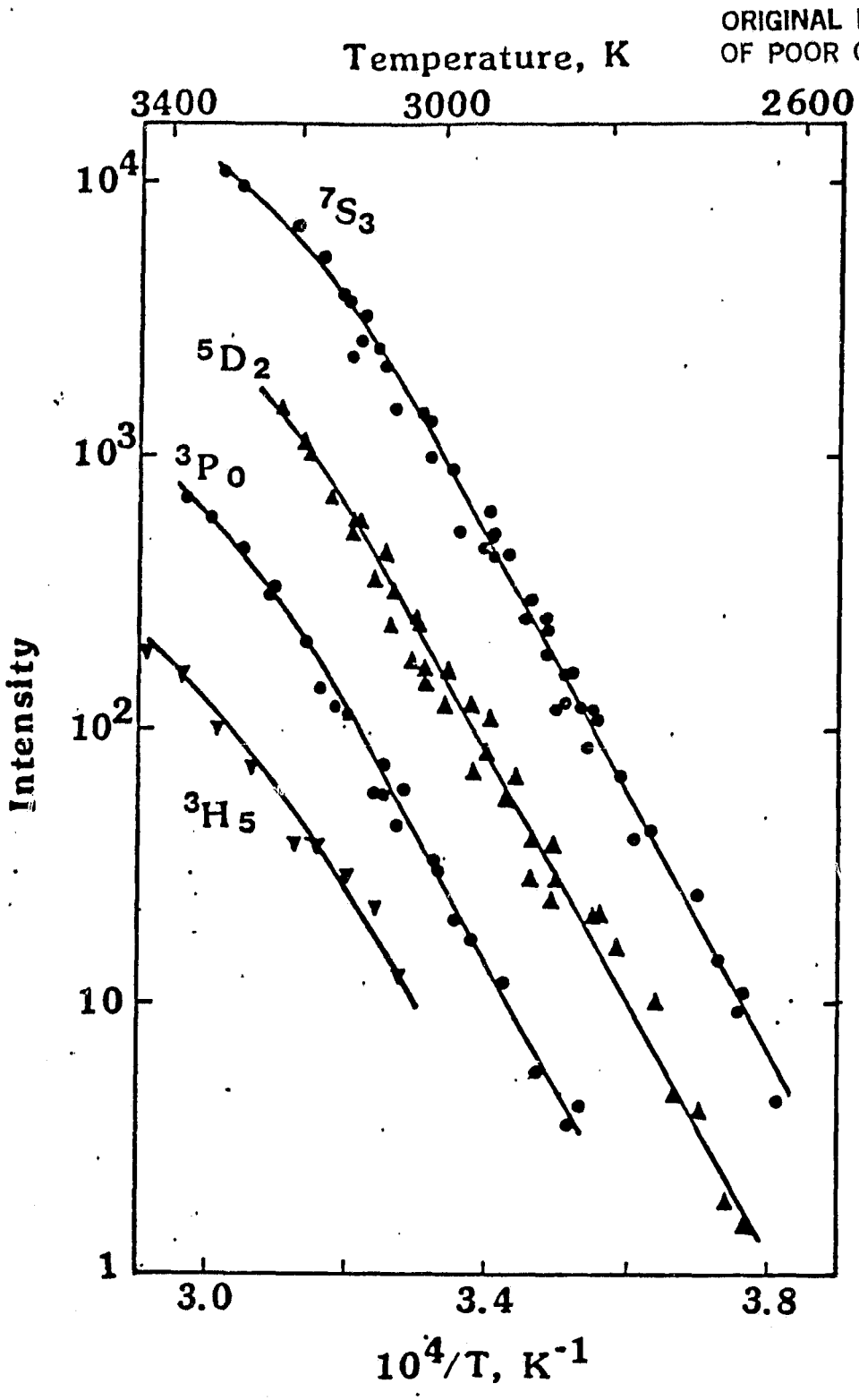

Figure 13. Temperature Dependence of Fluorescence Intensity for Four Metastable States of Atomic Tungsten.